IAC-13, A2.3, 10x18383

Numerical Simulations in preparation of a low gravity experiment onboard REXUS 16: Chemical Wave In Soret Effect (CWIS)

Pugliese, A.
Università degli Studi di Napoli Federico II & Stevens Institute of Technology

Tzevelecos, W. - Runge, W. - Desenfans, O. - Galand, Q. - Van Vaerenbergh, S.
Université libre de Bruxelles

De Filippis, L. - Manzone, S. - Mancino, F
Universtá degli Studi di Napoli Federico II

The purpose of the CWIS experiment is to visualize the chemical wave due to thermodiffusion in a liquid binary mixture. The chemical wave is represented by a strong concentration gradient given by thermodiffusion at the beginning of the process. The milligravity condition will allow to clearly see the effect in the mixture composed by water and ethylene glycol. This effect cannot be visualized on ground since it is masked by buoyancy. The concentration of each component of the mixture will be measured using a Fizeau interferometer. The very beginning of the phenomenon has never been observed experimentally, but S. Vaerenbergh and J. C. Legros in 1990 gave an analytical demonstration of the enhancing of the process at the boundaries during its initial phase. The experiment will be performed during the REXUS 16 campaign in Kiruna (Sweden) in March 2014.

This paper shows the results of the numerical design process of the experiment. In order to clearly see what happens at the beginning of the process we should set the velocity of the image acquisition system according to the velocity of the process. Since the components of the mixture are fixed (and also their initial concentration) the main parameters that are affecting the velocity of the Soret effect are the intensity of the temperature gradient and the dimension of the liquid volume along the gradient direction. A large campaign of numerical simulations allowed to determine suitable values for this parameters, in order to clearly see the variation of concentration due to thermodiffusion.

Keywords: Thermodiffusion, Soret Effect, Low Gravity

I. INTRODUCTION

The effect that causes molecules to move along temperature gradients is called thermodiffusion or, in case of liquid mixtures, Soret diffusion. This phenomenon causes the species with the lower molecular mass to migrate towards the zone with the higher temperature and the heavier molecules to move oppositely towards the colder zone. For this reason the separation due to Soret diffusion remains small [1]. Thanks to the gravity field the temperature gradient induces also buoyancy which tends to separate the species. It can be either compliant or opposite to the thermodiffusive effect according to the direction of the temperature gradient with respect to the gravity acceleration and the sign of the Soret coefficient.

The purpose of the CWIS Experiment is to show what happens to a binary mixture made up of ethylene glycol and water when subject to a thermal gradient. In order to visualize only the Soret effect, avoiding the buoyancy effect, we decided to use a low-gravity platform. The experiment is focused on the very beginning of the thermodiffusion. It has been theoretically predicted that during the initial phase the process is enhanced due to boundary effects.

According to the low-gravity period duration and the gravity disturbances level needed for the success of the experiment, among all the low-gravity platforms provided by ESA and available for European scientists, a sounding rocket has been selected. Since the team is entirely made up of students there was the chance to enter a student program like REXUS: Rocket-borne EXperiments for University Students.

A. The REXUS/BEXUS Programme

The REXUS/BEXUS programme is realised under a bilateral Agency Agreement between the German Aerospace Center (DLR) and the Swedish National Space Board (SNSB). The Swedish share of

the payload has been made available to students from other European countries through a collaboration with the European Space Agency (ESA). EuroLaunch, a cooperation between the Esrange Space Center of SSC and the Mobile Rocket Base (MORABA) of DLR, is responsible for the campaign management and operations of the launch vehicles. Experts from ESA, SSC and DLR provide technical support to the student teams throughout the project [2].

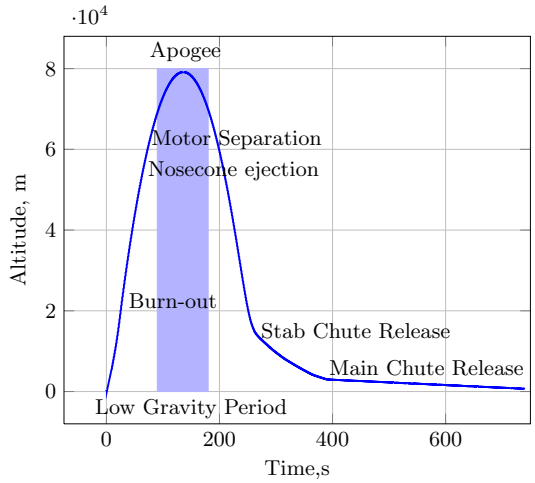

Figure 1. Typical REXUS flight profile with low gravity period and main mission activities indicated

The launch campaign is scheduled to be in March 2014 at the Esrange Space Center.
Figure 1 shows the flight profile of a typical REXUS mission. The apogee of the rocket trajectory is at least 80 kilometers and the low-gravity period duration is around 90 seconds.

B. The CWIS Payload

The CWIS experiment is going to investigate the behavior of a binary liquid mixture at the very beginning of the thermodiffusion process. Using a Fizeau interferometer the payload will record the refractive index changes that will happen in the mixture. The data coming from the experiment will later be analyzed and used to determine the mass fraction of each species inside the liquid cell.

Figure 2 shows the structural connection system and the arrangement of the internal components. The payload is connected to the rocket with a dampers system that will soften the initial launch acceleration and will isolate the internal components from vibrations. The payload structure is a closed cylindrical box entirely made of aluminum alloy with a polyurethane layer that will work as thermal insulator and will contain liquids in case of leaks. In figure 2 the top cover has been removed.

Figure 2. Experiment: 1. Laser, 2. Microscopic Objective, 3. Mirror, 4. Collimating Lens, 5. Beam Splitter, 6. Liquid Cell, 7. Spherical Lens, 8. First Cylindrical Lens, 9. Second Cylindrical Lens, 10. Camera, 11. Electronics, 12. Damping Springs, 14. Feed Through Cable Bracket

The internal components of the payload are grouped in three subsystems:

- the liquid cell contains the liquid mixture that is going to be studied. It is made up of a quartz cell, two copper plates at the top and bottom of the cell and a pressure compensation chamber. A heater is placed above the copper plate to establish the temperature gradient inside the liquid mixture;

- the interferometer subsystem will allow the measurement of the density of the mixture inside the liquid cell. It is made up of a laser, a camera and several optical components to enlarge the resolution along the thermal gradient. Since the interest if focused on the beginning of thermodiffusion and on the boundary effect the Field of View of the interferometer is few millimeters within the hot zone of the cell;

- the electronics subsystem takes care of the execution of each task during the mission. It controls the temperature of the heater the image acquisition from the camera and it receives the commands from ground.

Since the liquid cell is both an optical element and the container of the liquid mixture its design process includes both optical and fluid dynamics considerations. Although in this paper only the fluid dynamics side of the design is shown.

C. Liquid Mixture

Thermodiffusion in liquid mixtures is not well understood theoretically. For liquids with specific interactions such as hydrogen bonds it is often not even possible to predict the behavior correctly [3]. It is not always true that the species with the lower molar mass migrates towards the hotter zone, not even in binary mixtures.

The liquid inside the quartz cell is a mixture made up of 99% ethylene glycol and 1% water (mass percentage). After the launch campaign the experiment results will be compared with the numerical simulations in order to validate the assumptions made in the preparation phase.

II. EQUATIONS OF THE PROBLEM

The starting point are the Navier-Stokes Equations

$$\frac{1}{\rho}\frac{D\rho}{Dt} + \nabla\cdot\mathbf{V} = 0 \tag{1a}$$

$$\rho\frac{D\mathbf{V}}{Dt} + \nabla p = \nabla\cdot\underline{\underline{\tau}}_{\nu} + \rho\mathbf{g} + \mathbf{f}_b \tag{1b}$$

$$\rho\frac{Dh}{Dt} - \frac{Dp}{Dt} = -\nabla\cdot\mathbf{j}_q + \phi^2 + p\nabla\cdot\mathbf{V} + \dot{q}_h + L_b \tag{1c}$$

$$\rho\frac{Dc_i}{Dt} = \nabla\cdot\mathbf{j}_i + \rho\dot{c}_i \tag{1d}$$

where ρ is the density, $\mathbf{V}$ the velocity vector, p the static pressure, $\underline{\underline{\tau}}_{\nu}$ the viscous stress tensor, $\mathbf{g}$ the gravitational acceleration, $\mathbf{f}_b$ the body forces, h the specific enthalpy, $\mathbf{j}_q$ the heat flux, ϕ^2 the heat generated by viscous dissipation, $\dot{q}_h$ the heat generated from other forms of energy, L_b the work per unit time done on the fluid by the body forces, c_i the mass fraction of the i^{th} species, $\mathbf{j}_i$ its flux and $\dot{c}_i$ its production.

The momentum, energy and species diffusive fluxes are represented using the phenomenological equations

$$\underline{\underline{\tau}}_{\nu} = \mu\nabla\mathbf{V} \tag{2a}$$

$$\mathbf{j}_q = -\lambda\nabla T + L_{Qi}\nabla c_i \tag{2b}$$

$$\mathbf{j}_i = L_{iQ}\nabla T - \rho D_i\nabla c_i \tag{2c}$$

in which, except for the Newton's relation, the other two diffusive fluxes are expressed in a more general way in order to take into account the cross terms between heat diffusion and species diffusion. In the equations (2) μ is the kinematic viscosity, λ the thermal conductivity, D_i the diffusivity of the i^{th} species and L_{iQ} and L_{Qi} the Onsager coefficients.

No forces other than gravity are supposed to act on the fluid, so $\mathbf{f}_b = \mathbf{0}$ and the work they perform $L_b = 0$. The velocities are supposed to be very small, so the heat generated by viscous dissipation ϕ^2 will be neglected. Within the fluid there are no energy sources, so the term $\dot{q}_h$ is negligible. The mixture is supposed in absence of chemical reaction, so there will be no production of species $\dot{c}_i$. The coefficients μ, λ, D_i, L_{Qi} and L_{iQ} are supposed to be constant with time. The density ρ is also supposed to be constant except for the momentum equation in which the Boussinesq assumption is assumed to be valid

$$\rho = \rho_0[1 + \beta_T(T - T_0) + \sum_{i=1}^{N-1}\beta_{ci}(c_i - c_{0i})] \tag{3}$$

where β_T is known as the thermal expansion coefficient and β_{ci} expresses the density variation with the concentration of each species. Figure 3 shows the variation of the density with the temperature and the mass fraction of water. The two coefficients are reported in table I together with other liquid properties.

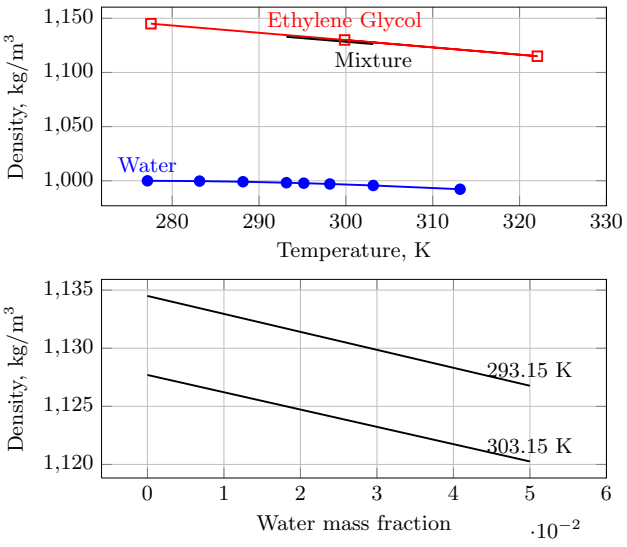

Figure 3. Density of the mixture vs temperature and water mass fraction. The trend of water density over temperature is assumed to be linear within the temperature range of interest. The mixture density is evaluated considering a water mass fraction of 0.01.

At the reference state in which $\mathbf{V} = 0$ in the entire flow field the momentum equation yields to the

Table I. Liquid properties

	Units	**Symbol**	**Water**	**Ethylene Glycol**
Density	$\mathrm{kg/m^3}$	ρ	997.6	1134.4
Specific Heat	$\mathrm{J/kg\,K}$	c_p	4182	2415
Molar Mass	g/mol	m	18.0152	64.0482
Viscosity	$\mathrm{kg/m\,s}$	μ	0.001	0.0157
Thermal Conductivity	$\mathrm{W/m\,K}$	λ	0.6	0.252
				Mixture
Mass Diffusivity	$\mathrm{m^2/s}$	D		1.00×10^{-9}
Soret Number	1	So		1.00×10^{-3}
Thermal Expansion Coefficient	1/K	β_T		-0.6684
Chemical Expansion Coefficient	1	β_c		-154.6

definition of the hydrostatic pressure $\nabla p_h = \rho_0 \mathbf{g}$.

Within these hypotheses the equations of the problem are

$$\nabla \cdot \mathbf{V} = 0 \tag{4a}$$

$$\begin{aligned}\frac{\partial \mathbf{V}}{\partial t} + (\mathbf{V}\cdot\nabla)\mathbf{V} = &-\frac{1}{\rho_0}\nabla(p-p_h)+\\ &+\nu_0\nabla^2\mathbf{V}+\\ &+\mathbf{g}[\beta_T(T-T_0)+\\ &+\beta_c(c-c_0)]\end{aligned} \tag{4b}$$

$$\begin{aligned}\frac{\partial T}{\partial t} + \mathbf{V}\cdot\nabla T = &\frac{1}{\rho_0 c_p}\frac{\partial p}{\partial t} + \frac{1}{\rho_0 c_p}\mathbf{V}\cdot\nabla p +\\ &+\alpha_0\nabla^2 T + \frac{L_{Q1}}{\rho_0 c_p}\nabla^2 c\end{aligned} \tag{4c}$$

$$\frac{\partial c}{\partial t} + \mathbf{V}\cdot\nabla c = \frac{L_{1Q}}{\rho_0}\nabla^2 T + D_0\nabla^2 c \tag{4d}$$

where the momentum diffusivity $\nu_0 = \mu_0/\rho_0$, the thermal diffusivity $\alpha_0 = \lambda_0/\rho_0 c_{p0}$ and the species diffusivity D_0 evaluated at the reference time have been introduced. Since the fluid is a binary mixture, c represents the mass fraction of the lighter species and L_{Q1} and L_{1Q} the Onsager coefficients. These two coefficients are related to the Dufour and to the Soret effect, respectively.

The second Onsager coefficient can be expressed as

$$L_{1Q} = D_T \rho_0 c(1-c)T \tag{5}$$

while the first one is going to be neglected.

A. Non-dimensionalization

We can rewrite the equations (4) in a non-dimensional form. For spatial variables the reference value is the height H of the liquid volume, therefore the non-dimensional variables are

$$x^* = \frac{x}{H}, \qquad y^* = \frac{y}{H}, \qquad z^* = \frac{z}{H} \tag{6}$$

where according to figure 4 the non-dimensional coordinates are $-w/2 \le x^* \le w/2$, $-l/2 \le y^* \le l/2$ and $0 \le z^* \le 1$.

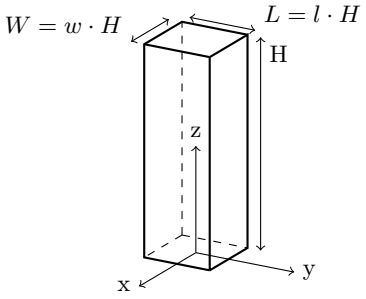

Figure 4. Geometry of the Liquid Volume

All the components of the velocity vector have been non-dimensionalized with the same reference value

$$V^* = \frac{V}{V_{\mathrm{ref}}} \tag{7}$$

where

$$V_{\mathrm{ref}} = \frac{\mathrm{Gr}}{H}\nu_0 \qquad \text{and} \qquad Gr = \frac{g\beta_T H^3}{\nu_0^2}T_{\mathrm{ref}}. \tag{8}$$

The Grashof number has been chosen instead of the usual Rayleigh number since it contains only the momentum diffusivity. This choice allowed to isolate the role of the thermal diffusivity inside the Prandtl number and the one of the species diffusivity in the Schmidt number

$$Pr = \frac{\nu_0}{\alpha_0}, \qquad Sc = \frac{\nu_0}{D_0}. \tag{9}$$

The non-dimensional pressure is defined as

$$p^* = \frac{p}{p_{\mathrm{ref}}} \qquad \text{where} \qquad p_{\mathrm{ref}} = \frac{1}{2}\rho_0 V_{\mathrm{ref}}^2 \tag{10}$$

The non-dimensional temperature is defined as

$$T^* = \frac{T - \overline{T}}{T_{\text{ref}}} \tag{11}$$

with

$$\overline{T} = T_C \qquad \text{and} \qquad T_{\text{ref}} = \Delta T \tag{12}$$

where ΔT is the temperature difference between T_H, the temperature at the hot wall and T_C, the one at the cold wall. The choice of $\overline{T}$ is due to the fact that the initial temperature of the whole mixture is equal to T_C.

The non-dimensional mass fraction of the species is

$$c^* = \frac{c - \overline{c}}{c_{\text{ref}}} \qquad \text{where} \qquad c_{\text{ref}} = \frac{L_{1Q} T_{\text{ref}}}{\rho_0 D_0} \tag{13}$$

and $\overline{c}$ is the initial concentration of the species.

The non dimensional time is

$$t^* = \frac{t}{t_{\text{ref}}} \tag{14}$$

where a different time reference has been chosen for each equation

$$t_{\text{ref}} = \frac{H^2}{\nu_0}, \qquad t_{\text{ref}} = \frac{H^2}{\alpha_0}, \qquad t_{\text{ref}} = \frac{H^2}{D_0} \tag{15}$$

in order to modify the obtained solution.

The non-dimensional equations are

$$\nabla^* \cdot \mathbf{V}^* = 0 \tag{16a}$$

$$\begin{aligned} \frac{\partial \mathbf{V}^*}{\partial t^*} = &- \text{Gr } (\mathbf{V}^* \cdot \nabla^*)\mathbf{V}^* + \\ &- \frac{\text{Gr}}{2} \nabla^* (p^* - p_h^*) + \\ &+ {\nabla^*}^2 \mathbf{V}^* + \mathbf{g}^* (T^* - T_0^*) + \\ &+ \text{So } \mathbf{g}^* (c^* - c_0^*) \end{aligned} \tag{16b}$$

$$\begin{aligned} \frac{\partial T^*}{\partial t^*} = &- \text{Gr Pr } (\mathbf{V}^* \cdot \nabla^*) T^* + \\ &+ \frac{\nu_0^2}{2 c_p T_{\text{ref}} H^2} \text{Gr}^2 \frac{\partial p^*}{\partial t^*} + \\ &+ \frac{\nu_0^3}{2 c_p T_{\text{ref}} H^2 \alpha_0} \text{Gr}^3 \ \mathbf{V}^* \cdot \nabla^* p^* + \\ &+ {\nabla^*}^2 T^* \end{aligned} \tag{16c}$$

$$\begin{aligned} \frac{\partial c^*}{\partial t^*} = &- \text{Gr Sc } (\mathbf{V}^* \cdot \nabla^*) c^* + \\ &+ {\nabla^*}^2 T^* + {\nabla^*}^2 c^* \end{aligned} \tag{16d}$$

where the separation parameter So is defined as

$$\text{So} = \frac{\beta_c L_{1Q}}{\beta_T \rho_0 D_0} T_{\text{ref}} \tag{17}$$

and the Soret number is

$$\text{S} = \frac{D_T}{D_0}. \tag{18}$$

Table II. Experiment conditions

	Units	Value
Gravity acceleration	m/s^2	0
Cell width	m	10×10^{-3}
Cell length	m	10×10^{-3}
Cell height	m	30×10^{-3}

B. Experiment Conditions

According to the principles of order of magnitude analysis explained in [4] and the experiment conditions showed in table II the equations of the problem are

$$\nabla^* \cdot \mathbf{V}^* = 0 \tag{19a}$$

$$\begin{aligned} \frac{\partial \mathbf{V}^*}{\partial t^*} = &{\nabla^*}^2 \mathbf{V}^* + \mathbf{g}^* (T^* - T_0^*) + \\ &+ \text{So } \mathbf{g}^* (c^* - c_0^*) \end{aligned} \tag{19b}$$

$$\frac{\partial T^*}{\partial t^*} = {\nabla^*}^2 T^* \tag{19c}$$

$$\frac{\partial c^*}{\partial t^*} = {\nabla^*}^2 T^* + {\nabla^*}^2 c^* \tag{19d}$$

III. RESULTS

The equations (19) have been solved using Fluent 6.

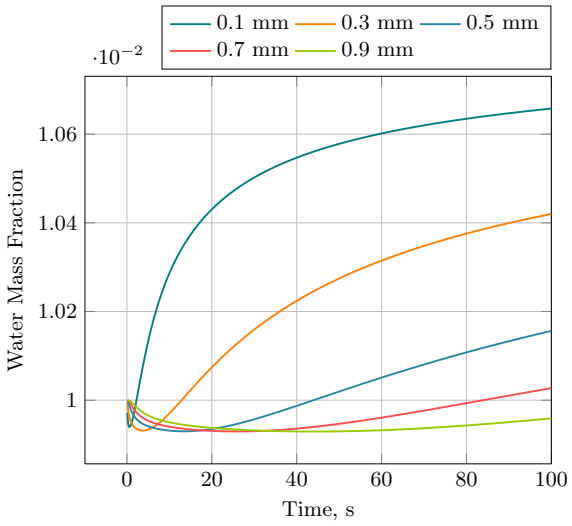

Figure 5. Water mass fraction over time in no gravity condition, 10 K temperature difference at different distances from the hot wall

Figure 5 shows the mass fraction of water during the first 100 seconds at five different distances from

the hot wall. Since the experiment is focused on the very fist seconds of the profecc, figure 6 shows what happens during the first ten seconds at the same five stations. The thermodiffusion effect causes the migration of water towards the hot wall, which leads to the decrease of water mass fraction in the downstream zone.

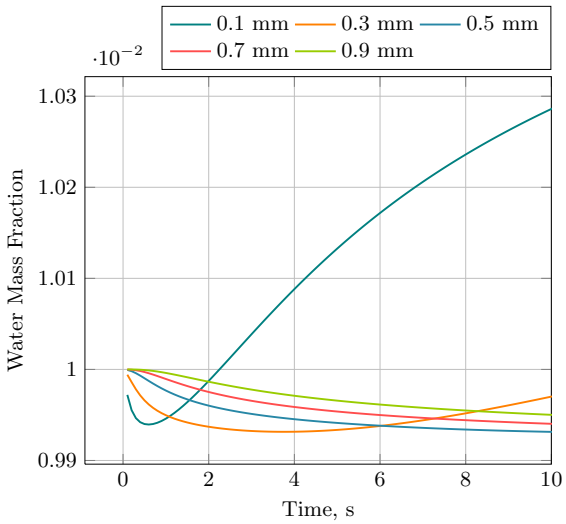

Figure 6. Water mass fraction over time in no gravity condition, 10 K temperature difference at different distances from the hot wall

A. The Chemical Wave

The chemical wave is a theoretical construct used to express the idea of chemical specie traveling along the fluid. In analogy with a pressure wave, where the driving force is the pressure gradient and the effect is the momentum variation, in the chemical wave in the case of thermodiffusion the driving force is the temperature gradient and the effect is the variation of mass fractions.

While the pressure wave can be described using only the momentum equation, the chemical wave due to thermodiffusion needs both the energy balance and the species balance equation. The driving force is a temperature gradient and it is described using the energy balance equation, while the effect is the mass fraction variation which is described by the species balance equation.

From equations (19) we see that the driving force propagates using the simple Fourier diffusion. Differently the migration of water molecules towards the hot wall causes a decrease in the downstream region. This minimum of mass fraction causes both and adverse concentration gradient which counteracts the thermodiffusion process and a concurrent concentration gradient on the other side which tends to enhance the phenomenon.

In order to show the propagation of the information within the fluid the time at which the minimum of the water concentration occurs at a certain station has been plotted in figure 7. The parabolic-like shape of the curve suggests that the velocity of the phenomenon is increasing with time.

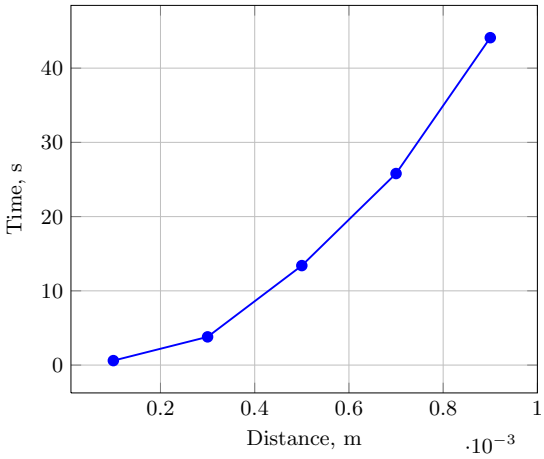

Figure 7. Time and position of the minimum of water mass fraction within the liquid mixture

B. Cell Design Process

The main requirement of the liquid cell is to allow the visualization of the chemical wave. The design process included all the optical characteristics and the influence they may have on the image quality, the dimensions constraints and the structural loads acting in the cell. From the fluid dynamics point of view the main parameters are the temperature difference and the distance between the two walls.

1. *Temperature Influence*

Figure 8 shows the effect of temperature on the intensity of the process. As expected a larger temperature difference increases the thermodiffusion effect. The increase is almost linear with temperature difference.

Figure 9 shows the effect of the temperature difference on the velocity of the process. The edgy shape of the curves is due to the time discretization, but the effect of the temperature difference is clearly visible. The higher the temperature gradient, the faster the chemical wave.

Considering the small effect on the velocity of the process and the interconnections with the other sub-

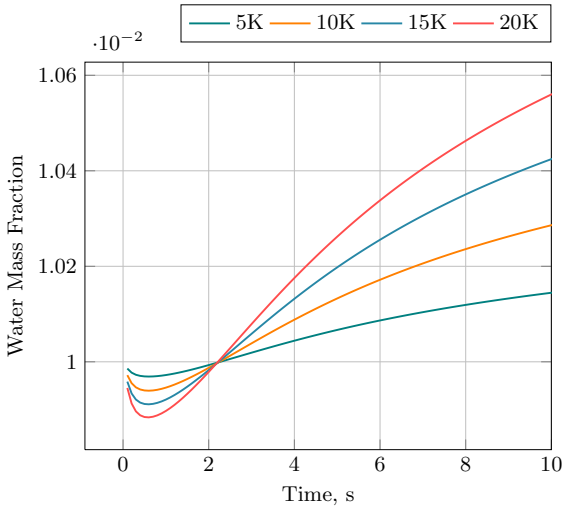

Figure 8. Water mass fraction over time in 0-gravity condition, at different temperature differences and at 0.1 mm from the hot wall

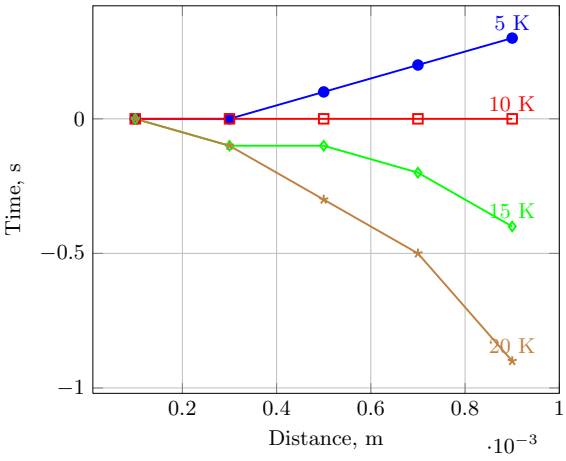

Figure 9. Time difference between reference case and others at various temperature differences: 5 K, 15 K, 20 K

systems like the electrical power required to set the temperature gradient the optimal value for the temperature difference was found to be 10 K. With this value the effect on the water mass fraction change is adequate to the interferometer performances.

2. *Length Influence*

As shown in equations (19) thermodiffusion depends on the temperature gradient and so on the temperature difference and on the distance between the two plates. The cell has got an initial temperature which is equal to the environment temperature. At the beginning of the low-gravity period, on one plate the heater starts to heat up the cell until the desired temperature difference between the plates is achieved. Obviously the system will need a certain time to have a linear temperature distribution. This time is proportional to the length of the cell. The value of 30 mm has been found to be the best one to slow down the thermodiffusion process in order to clearly see it with the coarse time resolution of the interferometer.

3. *Gravity Influence*

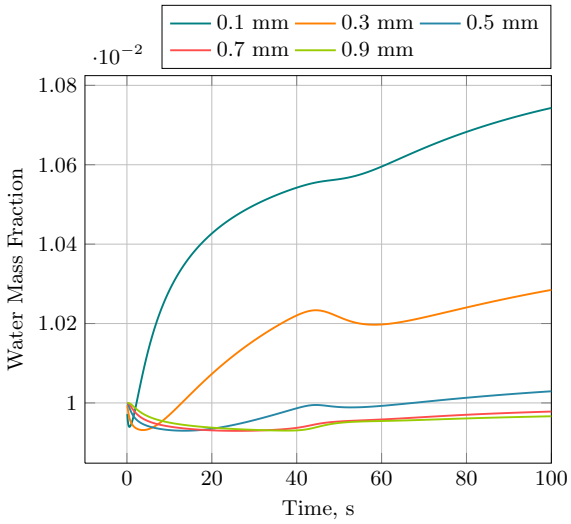

Figure 10. Water mass fraction over time in ground gravity condition at different distances from the hot wall

The effect of the gravitational acceleration on the thermodiffusion process is shown in figure 10. The curves clearly show that the larger influence occurs at larger distances from the wall. This is due to the velocity of the fluid. After a certain time the driving force, which in the thermodiffusion process is the temperature gradient, induces the migration of molecules. This leads to momentum transport which gets influenced by gravity. The effect is small near the wall and at the very beginning of the process.

IV. CONCLUSIONS

This paper shows a numerical simulation campaign in preparation to a sounding rocket experiment on board the REXUS 16. The CWIS Team is composed by Belgian and Italian students from different Universities which applied for the REXUS-BEXUS programme in 2012. The CWIS experiment core is a Fizeau interferometer designed to investi-

gate the thermodiffusion effect in a very small region. This allows to study the very beginning of this phenomenon which was never been observed but only theorized. What we expect is a Chemical Wave consisting in a concentration variation due to thermodiffusion effect which is very strong in the very beginning when the thermal gradient apply. Before the experimental application, we performed numerical simulation in order to understand the relation between thermodiffusion with all the parameters which characterize the experimental set-up as temperature and liquid cell dimension. The temperature difference selected for the experimental application is 10K along a cell dimension of $10x10x30$mm, where the dimension along the thermal gradient is the greater one. Numerical simulation are needed especially to set camera parameters as frame rate acquisition and initial fringe spacing. All these parameters are chosen to obtain the best signal resolution when the data will be processed. This paper shows also a theoretical order of magnitude analysis allowed to understand the importance of each term and to focus on the most prominent ones. Non-dimensional analysis allows to obtain references times which are used to size the system under investigation. From the simulation performed in 0-gravity condition, the phenomenon is more evident in a fraction of a millimeter from the hot side of the system. This explain the use of a modified Fizeau interferometer with cylindrical lenses to zoom on the region of interest. To assess the possibility of this application on the REXUS sounding rocket, we performed simulation in ground gravity condition to show as the milligravity condition of the sounding rocket doesn't affect the phenomenon. Further interpretations will be given after the launch campaign when the numerical results shown in this paper will be compared with the experimental results.

[1] Van Vaerenbergh, S. - Legros J.C., *Kinetics of the Soret Effect: Transient in the Transport Process*, Physical Review A 41.12 (1990)

[2] Fittock, M., *REXUS User Manual*, EuroLaunch (2012)

[3] Kita, R. - Wiegand, S. - Luettmer-Strathmann, J., *Sign change of the Soret coefficient of polyethylene oxide in water/ethanol mixtures observed by thermal diffusion forced Rayleigh scattering*, Journal of Chemical Physics, Vol. 121, No. 8 (2004)

[4] Monti, R., *Physics of Fluids in Microgravity*, Earth Space Institute Book Series (2002)

[5] Henry, D., *Simulation Numerique 3D des Mouvements de Convection Thermosolutale d'un Melange Binaire - Etude Parametrique de l'Influence de la Convection sur la Separation des Especes du Melanges par Effet Soret dans un Cylindre Incline*, (1986)

[6] Eslamian, M., *Advances in Thermodiffusion and Thermophoresis (Soret Effect) in liquid mixtures*, Frontiers in Heat and Mass Transfer 2 (2011)